

# FEMTOSECOND SYNCHRONIZATION AND STABILIZATION TECHNIQUES\*

J. Kim<sup>†</sup>, F. Ludwig<sup>‡</sup>, J. Chen, Z. Zhang<sup>§</sup> and F. X. Kärtner, MIT, Cambridge, MA 02139, USA.

## Abstract

High-precision synchronization and stabilization techniques are crucial for future advances in next generation light sources, seeded x-ray free electron lasers. In this paper, we present long-term stable femtosecond-precision optical-to-RF and optical-to-optical synchronization and stabilization techniques. For optical-to-RF synchronization, we demonstrate an optical-microwave phase detector that is capable of extracting an RF-signal from an optical pulse train in a long-term drift-free way. Extraction of an RF-signal with 3-fs in-loop timing jitter, integrated from 1 Hz to 10 MHz, from an optical pulse train is demonstrated. Optical-to-optical synchronization of two femtosecond lasers with sub-femtosecond precision over 12 hours is demonstrated. We also discuss how to use optically stabilized fiber links for timing distribution. Together with low-noise mode-locked lasers, a flexible femtosecond timing system can be constructed.

## INTRODUCTION

Seeding of free electron lasers operating in the x-ray regime with radiation generated from ultrafast laser sources, either directly, via nonlinear crystals, or via high harmonics from noble gases, may result in a fully coherent x-ray laser. For seeding of such large-scale facilities spanning over several hundreds meters to a few kilometers, it is critical to synchronize low-level RF-systems, photo-injector lasers, seed radiation and potential probe lasers with low timing jitter, preferably in sub-10-femtosecond range, in a long-term stable arrangement [1].

Figure 1 shows the schematic of the envisioned timing distribution and synchronization system for the future next generation light sources, seeded x-ray free electron lasers (XFELs). The pulse repetition rate of an optical master oscillator implemented as a mode-locked laser is stabilized to an optical and/or microwave frequency standard. The pulse train is distributed to all critical sub-systems, i.e., the pulsed klystron, the photo-injector laser, the low-level RF systems for linear accelerator, the seed laser as well as probe lasers, by use of timing stabilized fiber links. Finally, low-jitter, drift-free optical-to-RF and optical-to-optical synchronization between the distributed timing pulse trains and the remote RF- or optical sub-systems will result in a tightly synchronized timing system over the large-scale accelerator facility.

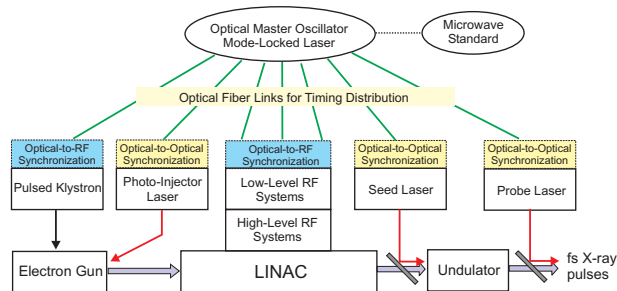


Figure 1: Schematic outline of timing distribution and synchronization for seeded X-ray free electron laser (XFEL) facilities.

Currently, the most promising candidates for ultra-low jitter optical master oscillators are passively mode-locked Er-doped fiber lasers [2], Yb-doped fiber lasers [3] and Er/Yb-glass lasers [4, 5]. Erbium and Ytterbium gain materials have long upper-state lifetime in the ms-range, and therefore, the high frequency fluctuations of the laser output in amplitude and timing are quantum noise limited [6]. Thus the timing jitter of mode-locked lasers is superior to that of conventional microwave oscillators in the high frequency range.

The crucial performance indicator for the optical master oscillator is the phase noise or timing jitter in the high frequency range. The bandwidth of optical/microwave reference locking is typically limited to tens of kHz range, and the high-frequency noise beyond locking bandwidth follows that of the free-running master oscillator. In addition, timing stabilization of fiber links based on the cross-correlation of the back-reflected pulse from fiber end with the fresh pulse also has a bandwidth limitation from the travel time of the reflected pulse. These limitations assure that a very low jitter mode-locked laser is a prerequisite for a high-precision timing system.

In Refs. [7] and [8], the timing jitter is characterized by measuring the phase noise of one harmonic (at 1.3 GHz) of the microwave signal obtained by direct photodetection of the pulse train. For standard Er-doped stretched pulse fiber lasers, the integrated timing jitter from 1 kHz to 22 MHz (Nyquist bandwidth) is measured on the order of 10 fs, which is already better than most commercial high-quality microwave signal generators (for example, Marconi 2041 signal generator). Note that the measurements are often limited in precision by the amplitude-to-phase (AM-to-PM) conversion from direct photodetection. A more detailed discussion on this conversion will be given in the next section. In theory, the high frequency timing jitter of pulse trains from mode-locked lasers can be below one femtosec-

\* Supported by ONR, AFOSR, and EUROFEL.

<sup>†</sup> jungwon@mit.edu

<sup>‡</sup> Permanent address: DESY, Hamburg, Germany

<sup>§</sup> Permanent address: Peking University, Beijing, China

ond.

Once a timing signal in form of an optical pulse train is generated from a master oscillator, it should be distributed to the remote RF- or optical-subsystems that we aim to synchronize with minimal excess noise. Precise transfer of timing signals through fiber links for timing information dissemination has been demonstrated recently [7, 9, 10, 11] for short time spans, typically less than a minute. If the fiber length is  $L$ , we assume that no length fluctuations are faster than  $2L/c$ , where  $c$  is the speed of light in the fiber. Relative fiber expansion by temperature change is typically on the order of  $10^{-7}/K$ , which can be compensated by a fiber length control loop by referencing the back reflected pulse from the fiber end with the later pulse from the mode-locked laser. Recently, the demonstration of timing distribution over 500 meters in an accelerator environment was done with pure RF-techniques [7]. When the feedback loop is open, the jitter integrated from 0.1 Hz to 5 kHz is 66 fs; when the loop is closed, the in-loop jitter is suppressed down to 12 fs. More detailed information on this timing distribution experiment can be found in Ref. [7].

Although a short-term stabilization on the order of few tens of femtoseconds can be achieved with RF-techniques only, for long-term stabilization of fiber links with sub-10 fs accuracy over hours, balanced cross-correlation techniques [12] can be employed, as discussed later in this paper. Work is in progress to demonstrate long-term stable fiber links.

## OPTICAL-TO-RF SYNCHRONIZATION

Once precise timing information encoded as an optical pulse train arrives at each remote location, the next task is to synchronize it with, for example, RF-subsystems. It is crucial to convert this optical signal into a low-jitter, drift-free RF-signal with a satisfactory power level in a long-term stable way. Recently, it has been shown that the extraction of an RF-signal from an optical pulse train using direct photodetection is limited in precision by excess phase noise [13]. The major contribution to this excess noise was identified to be the amplitude-to-phase (AM-to-PM) conversion in the photodetector. The intensity noise of the laser can be converted into a significant amount of phase noise and phase drift by this process. In Refs. [8] and [14], the AM-to-PM conversion factor was measured and it typically ranges 1 to 10 ps/mW depending on the bias and the bandwidth of the photodetector. The intensity noise of the delivered pulse train can be converted into a significant amount of excess timing jitter by this process. For a 12-GHz InGaAs photodetector at 6 V reverse bias that we tested, the AM-to-PM conversion factor was measured as 1.6 ps/mW [8]. For an Er-doped fiber laser with 0.03 %<sub>rms</sub> relative intensity noise (RIN), this may already result in 5-fs excess jitter when 10 mW of power is applied to the photodetector. In addition, direct photodetection has a limited extractable RF-power and signal-to-noise ratio (SNR) due to the damage threshold for the input optical power to the

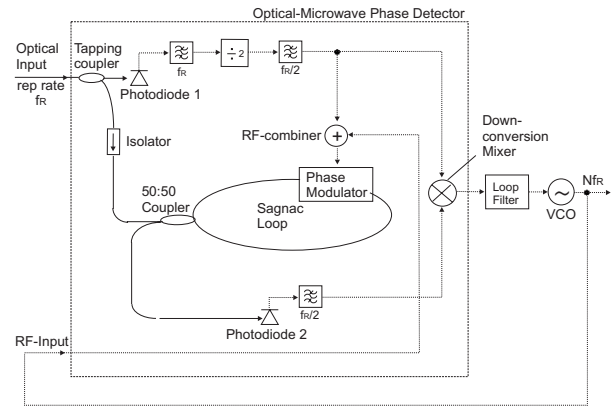


Figure 2: Schematic of a balanced optical-microwave phase detector and its use for RF-signal regeneration from an optical pulse train. VCO, voltage-controlled oscillator.

photodetector. Moreover, phase drifts in the diode due to temperature change as well as post-amplification to reach the required signal level can prevent a long-term stable regeneration of RF-signals.

Therefore, it is highly desirable to develop a phase-locked loop between an optical pulse train and a high-quality RF voltage-controlled oscillator (VCO) to prevent those undesired AM-to-PM conversion and drifts due to the photodetection process. In addition, one can leverage the fly-wheel effect of VCO. In doing so, the key issue is the development of drift-free, low-jitter phase detector which compares the relative phase between pulse trains and RF-signals in the optical domain before the photodetection is involved. Previously, we proposed and demonstrated a scheme to avoid the excess noise from direct photodetection by transfer of timing information in the optical domain [15]. However, due to acoustic vibrations and poor phase noise properties of the free-running VCO, the relative jitter was limited to 60-fs measured from 100 Hz to 10 MHz.

For the extraction of low-jitter, high-power, and drift-free RF-signals from optical pulse trains, a balanced optical-microwave phase detector is proposed and demonstrated. This phase detector is still based on the timing information transfer in the optical domain. The timing information transfer in the optical domain is implemented by use of a differentially-biased Sagnac fiber-loop and synchronous detection. We used the phase error signal from this balanced optical-microwave phase detector, which is robust against drifts and photodetector nonlinearities, to regenerate low-jitter RF-signals from optical pulse trains.

Figure 2 shows the schematic of the balanced optical-microwave phase detector. Part of the input pulse train is tapped off by Photodiode 1. This photodiode is used to generate a synchronous detection signal at half the repetition rate ( $f_R/2$ ) of the optical pulse source. This signal is applied to both the phase modulator and the down-conversion mixer. The rest of the input pulse train is sent to

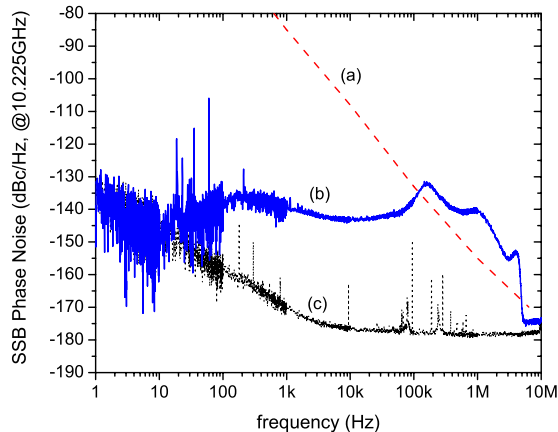


Figure 3: The single-sideband (SSB) phase noise spectra at 10.225 GHz. (a) Free-running VCO. (b) In-loop phase noise when it is locked. (c) Signal analyzer noise floor.

the Sagnac-loop with a phase modulator. The phase modulation in the Sagnac loop is converted into an amplitude modulated signal at  $f_R/2$  at the output of the Sagnac-loop. The amplitude of this signal is, to the first order, proportional to the phase error between the optical pulse train and the RF-signal (which is, the output from the VCO). The detected signal at Photodiode 2 is band-pass filtered at  $f_R/2$  and down-converted to the baseband by mixing with the reference signal. This error signal is filtered and controls the low-noise VCO to close the phase-locked loop.

For the demonstration experiment, a standard stretched-pulse Er-doped fiber laser [2] (repetition rate  $f_R = 44.26$  MHz) is used as the optical pulse source. All optical components in the phase detector are implemented using commercial 1550-nm optical fiber and components. In the experimental implementation, we generated a signal with the frequency  $10.5f_R$  for the phase modulation in the Sagnac-loop in parallel with  $f_R/2$  component to reduce the necessary fiber loop length. By closing the loop with a 10.225-GHz (231st harmonic of the fundamental repetition rate) VCO (PSI DRO-10.225), a long-term stable locking between the laser and the VCO is achieved.

Figure 3 shows the measured in-loop phase noise spectra at the output of down-conversion mixer. The voltage signal from the phase detector was amplified with a low-noise amplifier ( $G=10$  non-inverting amplifier with AD797) and measured with a low-noise vector signal analyzer (Agilent 89410A), and converted into single-sideband (SSB) phase noise at 10.225 GHz. This measurement shows that the integrated in-loop jitter is  $3.0 \text{ fs} \pm 0.2 \text{ fs}$  integrated from 1 Hz to 10 MHz when it is locked. Currently, the system is limited by the thermal noise from electronic amplifiers and has not yet reached shot noise limited performance yet. We are currently pursuing to further suppress the timing jitter to below 1 fs by increasing optical and RF power lev-

els as well as optimizing loop characteristics. In addition, the construction of a second loop is in progress to perform long-term out-of-loop measurements by mixing two VCO outputs in quadrature.

## OPTICAL-TO-OPTICAL SYNCHRONIZATION

Tight synchronization is necessary not only between optical and RF-subsystems but also between different optical systems, for example, the photo-injector laser, the seed laser and the probe lasers as shown in Fig. 1. Conventional timing synchronization between two mode-locked lasers based on microwave mixers [16] suffers from high residual jitter and thermal drifts in the electronic amplifiers and mixers. To overcome this limitations, a balanced optical cross-correlator [12] can be used for the long-term optical-to-optical synchronization. This technique uses nonlinear optical processes for an extremely sensitive detection of timing differences between optical pulses.

Figure 4 shows the schematic of the balanced cross-correlator. The combined pulses from two mode-locked lasers with different spectra, denoted as wavelengths  $\lambda_1$  and  $\lambda_2$ , are splitted by a broadband 50:50 beam splitter. The two beam paths have a different group delay (GD), for example, by inserting a glass plate in one of the arms. This group delay offsets the relative position between two pulses. Each combined pulse is focused into a nonlinear crystal to generate a sum-frequency component at  $\frac{1}{\lambda_{SFG}} = \frac{1}{\lambda_1} + \frac{1}{\lambda_2}$ . After bandpass filtering the sum-frequency generation (SFG) components, a balanced detector measures the intensity imbalance. For small timing differences (within the range of the group delay of the GD element), the output from the balanced detector is nearly proportional to the time difference between the two pulses. At the zero-crossing of the balanced detector output, the amplitude noise from each laser is balanced and does not affect the detected error signal. The signal from the balanced detector is used to lock the repetition rates of the two lasers by controlling the cavity length of one laser with cavity mirrors mounted on piezo-electric transducers (PZTs). This finally closes the loop. This method enables a drift-free and temperature-independent synchronization between two independent lasers.

The long-term timing synchronization performance using balanced optical cross-correlation is demonstrated using a 5-fs Ti:sapphire laser (centered at 830 nm) and a 30-fs Cr:forsterite laser (centered at 1250 nm). The pulses are combined and splitted by use of a broadband 50:50 beam splitter with matched group delay dispersion. LBO crystals with 1-mm thickness are used for SFG at 499 nm ( $1/830\text{nm} + 1/1250\text{nm} = 1/499\text{nm}$ ). To generate a group delay offset of 45 fs between 830 nm and 1250 nm, a 3-mm thick fused silica plate is used.

Figure 5 shows the out-of-loop cross correlation result for a timing jitter measurement between the Ti:sapphire and Cr:forsterite lasers. The black line shows the cross-

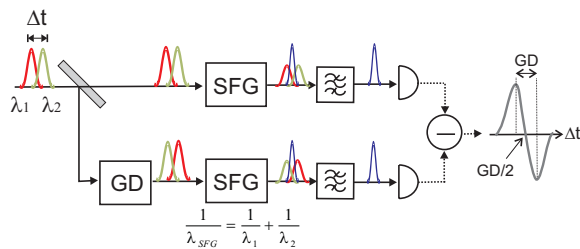


Figure 4: Schematic of a balanced cross-correlator. GD: group-delay element between two color pulses. SFG: sum-frequency generation.

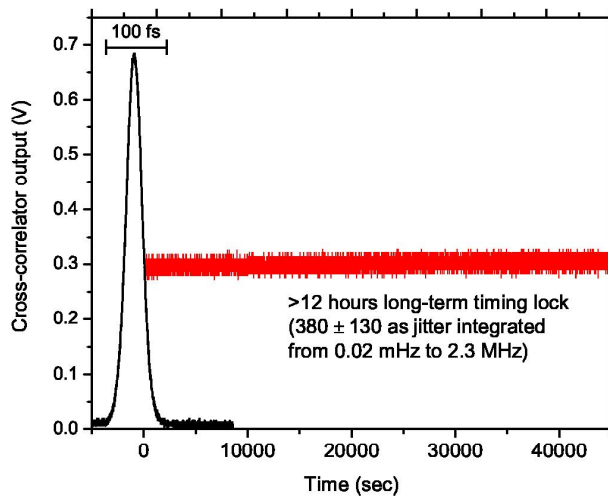


Figure 5: Long-term optical-to-optical synchronization result between Ti:sapphire and Cr:forsterite lasers. Drift-free sub-femtosecond synchronization over 12 hours were measured.

correlation trace when two lasers are not locked. The red line shows the cross-correlation trace when two lasers are locked adjacent to each other so that timing fluctuations are transferred into intensity fluctuations in the cross-correlation signal [16]. The pulse trains from the two lasers are locked with 380 attoseconds rms timing jitter over 12 hours without thermal drift in the bandwidth from 0.02 mHz to 2.3 MHz. Note that the duration of 12 hours does not constitute a limit to the locking scheme but was merely the duration of the experiment. In principle, as long as the lasers stay mode-locked, the timing lock can be maintained if the mechanical perturbations to the system are below a certain threshold value.

## CONCLUSION

In summary, we reported on the progress toward a long-term stable and scalable timing distribution and synchronization system for future accelerator and seeded x-ray free electron laser facilities proposed in Ref. [1]. In particular,

we demonstrated high-precision optical-to-RF and optical-to-optical synchronization techniques. We proposed and demonstrated the use of a balanced optical-microwave phase detector and balanced optical cross-correlator. By use of optical techniques, we could achieve a long-term femtosecond and sub-femtosecond accuracies which was not achievable with conventional pure RF-techniques.

## REFERENCES

- [1] J. Kim, F. Ö. Ilday, F. X. Kärtner, O. D. Mücke, M. H. Perrott, W. S. Graves, D. E. Moncton, T. Zwart, "Large-Scale Timing Distribution and RF-Synchronization for FEL Facilities," Proceedings of Free Electron Laser Conference 2004, p. 329, August 2004.
- [2] G. Lenz, K. Tamura, H. A. Haus and E. P. Ippen, *Opt. Lett.* **20**, 1289 (1995).
- [3] F. Ö. Ilday, J. R. Buckley, H. Lim, F. W. Wise and W. G. Clark, *Opt. Lett.* **28**, 1365 (2003).
- [4] J. B. Schlager, B. E. Callicoatt, R. P. Mirin, N. A. Sanford, D. J. Jones and J. Ye, *Opt. Lett.* **28**, 2411 (2003).
- [5] S. C. Zeller, L. Krainer, G. J. Spuhler, R. Paschotta, M. Golling, D. Ebling, K. J. Weingarten and U. Keller, *Electron. Lett.* **40**, 875 (2004).
- [6] S. Namiki and H. A. Haus, *IEEE J. Quantum Electron.* **33**, 649 (1997).
- [7] A. Winter, P. Schmöser, H. Schlarb, F. Ö. Ilday, J. Kim, J. Chen, F. X. Kärtner, D. Cheever, T. Zwart, D. Wang, "High-Precision Optical Synchronization Systems for X-Ray Free Electron Lasers," Proceedings of Free Electron Laser 2005, p. 676, August 2005.
- [8] F. X. Kärtner, F. Ö. Ilday, J. Kim, A. Winter, F. Grawert, H. Byun, J. Chen, "Progress in Large-Scale Femtosecond Timing Distribution and RF-Synchronization," Proceedings of 2005 Particle Accelerator Conference, p. 284, May 2005.
- [9] J. Ye, J. Peng, R.J. Jones, K.W. Holman, J.L. Hall, D.J. Jones, S.A. Diddams, J. Kitching, S. Bize, J.C. Bergquist, L.W. Hollberg, L. Robertsson, and L. Ma, *J. Opt. Soc. Am. B* **20**, 1459 (2003).
- [10] K. W. Holman, D. J. Jones, D. D. Hudson, J. Ye, *Opt. Lett.* **29**, 1554 (2004).
- [11] D. D. Hudson, S. M. Foreman, S. T. Cundiff and J. Ye, *Opt. Lett.* **31**, 1951 (2006).
- [12] T. R. Schibli, J. Kim, O. Kuzucu, J. Gopinath, S. N. Tandon, G. S. Petrich, L. A. Kolodziejewski, J. G. Fujimoto, E. P. Ippen, and F. X. Kärtner, *Opt. Lett.* **28**, 947 (2003).
- [13] E. N. Ivanov, S. A. Diddams and L. Hollberg, *IEEE J. Sel. Top. Quantum Electron.* **9**, 1059 (2003).
- [14] A. Bartels, S. A. Diddams, C. W. Oates, G. Wilpers, J. C. Bergquist, W. H. Oskay and L. Hollberg, *Opt. Lett.* **30**, 667 (2005).
- [15] J. Kim, F. X. Kärtner, and M. H. Perrott, *Opt. Lett.* **29**, 2076 (2004).
- [16] R. K. Shelton, S. M. Foreman, L. Ma, J. L. Hall, H. C. Kapteyn, M. M. Murnane, M. Notcutt and J. Ye, *Opt. Lett.* **27**, 312 (2002).